

# Evidences of methane-derived authigenic carbonates from the sediments of the Krishna–Godavari Basin, eastern continental margin of India

Kocherla Muralidhar\*, A. Mazumdar, S. M. Karisiddaiah, D. V. Borole and B. Ramalingeswara Rao

National Institute of Oceanography, Dona Paula, Goa 403 004, India

**Evidences of anaerobic oxidation of methane and interstitial carbonate precipitation have been recorded in sediment cores from Krishna–Godavari basin. High magnesian calcite and aragonite, typically associated with methane oxidation have been identified from the three studied cores. Down core sulphate reduction trend and presence of framboidal pyrites are definite evidences of anoxic diagenetic realm. Highly depleted carbon isotopic compositions of the handpicked carbonate crystals are suggestive of anaerobic oxidation of methane (AOM). In this work a biogenic methane source has been tentatively concluded. Presence of certain geophysical features, viz. bottom simulating reflector, gas charged sediments and pock-marked sea floor are suggestive of possible methane gas hydrate as methane source. However, an early diagenetic methane source is also a possibility in the present scenario. Further studies are in progress for comprehensive understanding of the processes involved.**

**Keywords:** Authigenic carbonate, gas-hydrate, Krishna–Godavari basin, methane, stable isotope.

PRESENCE of methane-derived authigenic carbonates within the sediment column and at the sediment surface has been described by several workers<sup>1–9</sup>. Precipitations of various carbonate mineral phases<sup>10,11</sup>, viz. calcite, aragonite, dolomite and siderite are brought about by the enrichment in pore water alkalinity. Enrichment in bicarbonate ion concentration has been attributed to anaerobic oxidation of methane (AOM) and concomitant sulphate reduction process<sup>12–16</sup> which can be represented by the equation:



AOM is believed to be performed by a consortium of CH<sub>4</sub>-oxidizing archaea and sulphate-reducing bacteria (SRB) in marine environments<sup>17,18</sup>.

AOM and precipitation of carbonates have been observed at a large number of locations with gas seepages and pore fluid ventings<sup>7,19</sup>. The carbonate precipitates<sup>20</sup> generally occur as individual slabs, thinly lithified pavements, vertical pillars, mushroom-like structures, microbial mats, dispersed crystals and as micro-concretions. The bicarbonate pool produced as a result of bacterial anoxic methane oxidation is significantly enriched in <sup>12</sup>C.

In the present work we report the occurrence of methane-derived disseminated authigenic carbonates in sedimentary cores from the Krishna–Godavari (KG) basin (eastern continental margin of India) and discuss the origin. This report is a part of a multidisciplinary programme under the aegis of NGHP on gas hydrate exploration in the eastern coast of India.

## Geological setting and sampling

The K–G basin is a pericratonic rift basin located in the middle of the eastern continental margin of Peninsular India<sup>21</sup>. The offshore extent of the KG basin is known to extend to a water depth at least 2000 m. Two major rivers, the Godavari and Krishna, supply the clastic load to the K–G basin. This basin comprises of a vast range of depositional settings such as coastal plains, deltas, shelf-slope aprons and deep-sea fans. Geophysical data indicates existence of a number of sub-basins and fault-controlled ridge-like structure with a NE–SW trend. The basal facies of the K–G basin is comprised of Palakollu shale (Paleocene), Vadaparru shale (Eocene), Narasapur claystone (Oligocene), Rawa Formation (Mio-Pliocene) and Godavari clay (Holocene–Pliostocene). Shallow marine and onshore succession is dominated by sandy sequences. The K–G basin has a sedimentary thickness of 5–7 km.

The study area lies within the continental slope region of eastern India (Figure 1). The seabed topography is characterized by relatively steep gradients. Several prominent ridges (200–300 m from the seafloor) were mapped at a depth of about 1400–1500 m. Major structural features in the region include NE–SW trending faults. Sediment

\*For correspondence. (e-mail: kocherla@nio.org)

cores selected for the present study are shown in Figure 1. The surveyed area is characterized by numerous gas-related features like pock-marks, vents, seepages, gas-masking and bottom simulating reflectors (BSRs)<sup>22</sup>.

## Analytical techniques

Sub-bottom profiler (ORE) was used for the study of shallow sub-surface features. An operational frequency of 3.5 kHz has provided a penetration of 30–50 m below sea bed. Sea water temperature, salinity and depth were measured using CTD profiler (SBE911, Sea Bird Electronics). Gravity cores of approximately 1–6 m were collected at specific sites. The sub-samples were collected at every 50 cm within 15–20 min after opening the core and were transferred to on-board laboratory for pore water extraction using a temperature controlled centrifuge (Heraeus-Biofuge). Pore waters in 25 ml airtight bottles were stored in refrigerators at  $-18^{\circ}\text{C}$  for onshore analyses of  $\text{SO}_4^{2-}$  concentrations using Dionex Ion-chromatograph, DX-600I. The degassing system fabricated by M. Schmitt from GCA, Germany (modified version<sup>23</sup>) was used for methane extraction from the sediment samples. Methane content was determined with a Carlo-Erba model CE-8000 TOP gas chromatograph. The total organic carbon (TOC) was estimated by chromic acid oxidation method<sup>24</sup>. Dried sediment samples were examined under binocular microscope (Nikon, P-FMD) for the presence of authigenic carbonates. The hand-picked carbonate fractions were first studied under scanning electron microscope (Jeol-JSM 5800 LV1) for the morphological classification of carbonate crystals. The same fraction was studied for carbonate mineralogy by X-ray diffractometry using Philips X-ray Diffractometer (PW-1840). Carbon and oxygen isotopic analyses were carried out by Europa Geo20-20

Stable isotope mass spectrometer at the Physical Research Laboratory, Ahmedabad. The isotopic compositions are expressed in the conventional  $\delta$  notation relative to the Pedee belemnite (PDB).

## Results

Sub-bottom profiler data show the presence of gas escape features, such as gas up-thrusts and pock mark-like features (Figure 2) on the basin floor. Bottom water temperature at the coring locations was  $\sim 4.5^{\circ}\text{C}$ . Locations of cores (GC-07, GC-10 and GC-13) are marked on Figure 1. Core length varies from 1.8 to 5.2 m. All the cores exhibit drop in sulphate concentration with depth. However, only for core GC-07 a complete sulphate concentration profile could be obtained which is presented here (Figure 3). This core shows methane concentration up to 153.5 nM and TOC content from 1 to 1.8%. Optical microscopic studies exhibit presence of sub-rounded calcareous patches of about 1 to 5 mm in the dried sediments of the cores.  $\delta^{13}\text{C}_{\text{PDB}}$  and  $\delta^{18}\text{O}_{\text{PDB}}$  of the carbonate crystals separated from these patches range from  $-51.6\text{‰}$  to  $-48.8\text{‰}$  and  $3.6\text{‰}$  to  $4.5\text{‰}$  respectively (Table 1).

The prominent carbonate patches were noticed in the sediments obtained from the depth interval of 225–230 cm in GC-07, 245–250 cm in GC-13, and 130–135 cm in GC-10. X-ray diffraction studies of these patches indicate high-Mg calcite (HMC) in core GC-7, GC-10 and aragonite in core GC-13. HMC commonly occurs as anhedral (Figure 4a) and euhedral (Figure 4b) crystals. Occasionally the HMC is of flaky nature (Figure 4c) with botryoids disseminated within it. Development of certain porous fabric possibly associated with gas diffusion through the sediments was noted at few places (Figure 4d). These pores are often filled with carbonates with botryoidal habit (Figure 4e). Aragonite occurs as radial fibrous, acicular

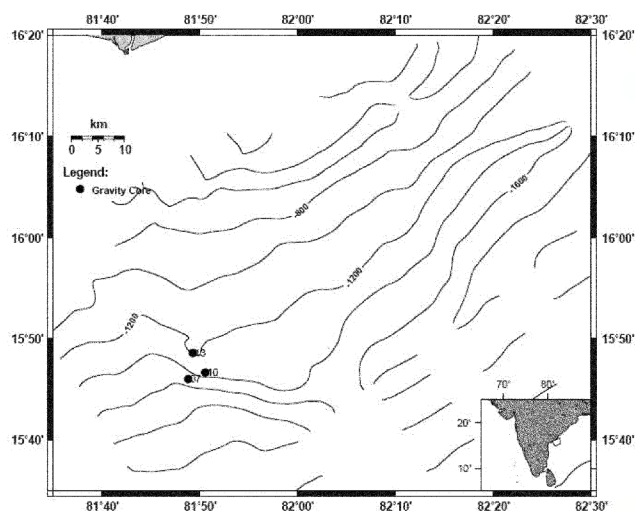


**Figure 1.** Bathymetry map of the part of Krishna–Godavari offshore basin. Solid circle indicate the gravity core locations.

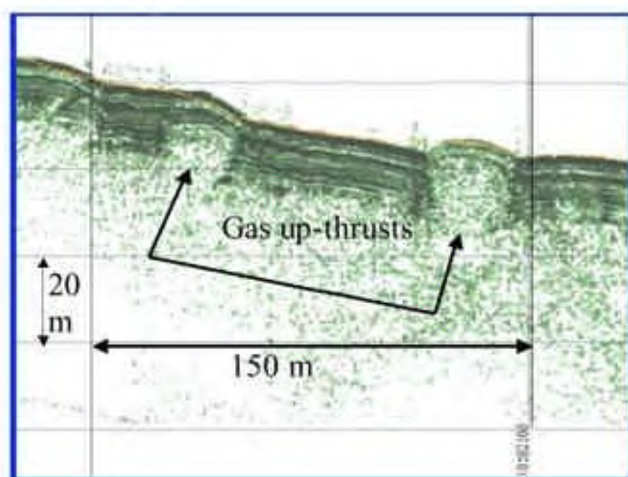


**Figure 2.** A typical gas up-thrust (gas escape features)-like structure near one of the core locations.

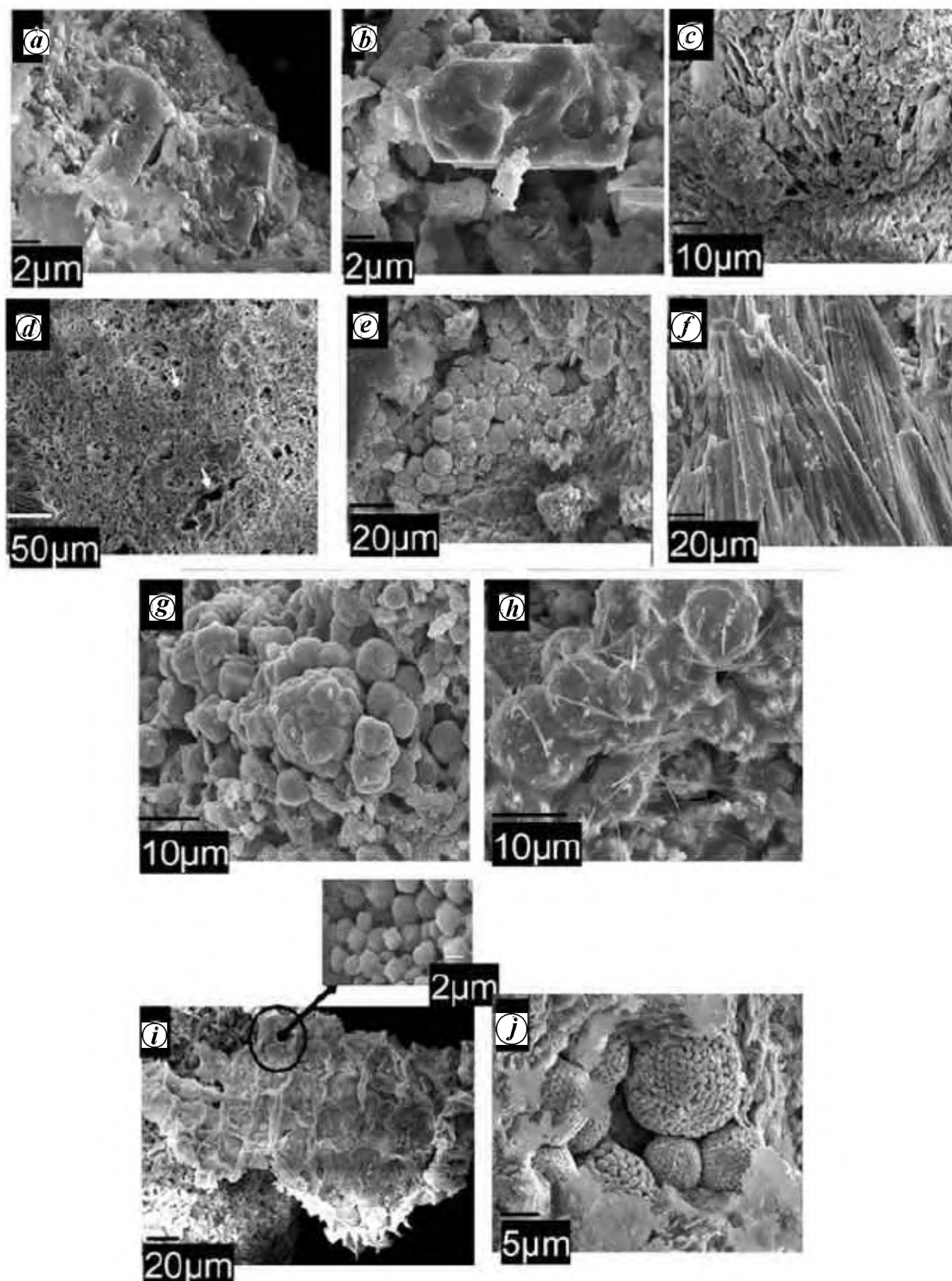


**Figure 3.** Scanning electron photomicrographs. *a*, Anhedronal crystals high magnesian calcite (GC-07); *b*, Euhedral crystals of high magnesian calcite (GC-07); *c*, Flaky high magnesian calcite with disseminated botryoids (GC-10); *d*, Porous fabric owing to gas effusion in figure 3 *d* (GC-13); *e*, Botryoidal aragonite precipitation within the pore spaces formed by gas effusion in figure 3 *d* (GC-13); *f*, Dense fabric of acicular aragonite crystals (GC-13); *g*, Botryoidal aragonite (GC-13); *h*, Growth of tender aragonite crystals on the botryoids; *i*, Remnant of biofilm-like feature with tiny rhomb shaped carbonate crystals (GC-13); *j*, framboidal pyrite within carbonates and clay matrix from anaerobic sediments (GC-10).

needle-like crystals (Figure 4*f*), and pore filling botryoids (Figure 4*g*). The aragonite appears as individual or clusters of needle-shaped crystals or occasionally as a dense fabric on the surfaces of foraminiferal test. Nucleations of needle-shaped aragonite crystals (Figure 4*h*) from 10-micron size botryoidal aragonite substrate were noted. Nearly 2 micron-sized rhomb-shaped crystals were associated with an apparent biofilm remnant (Figure 4*i*). About 5–20 micron size pyrite framboids are observed in isolation or in clusters (Figure 4*j*).

## Discussion

Geophysical observations<sup>22</sup>, evaluation of pore-fluid chemistry, mineralogical and isotopic studies of sediment cores from the K–G basin on the east coast of India collectively

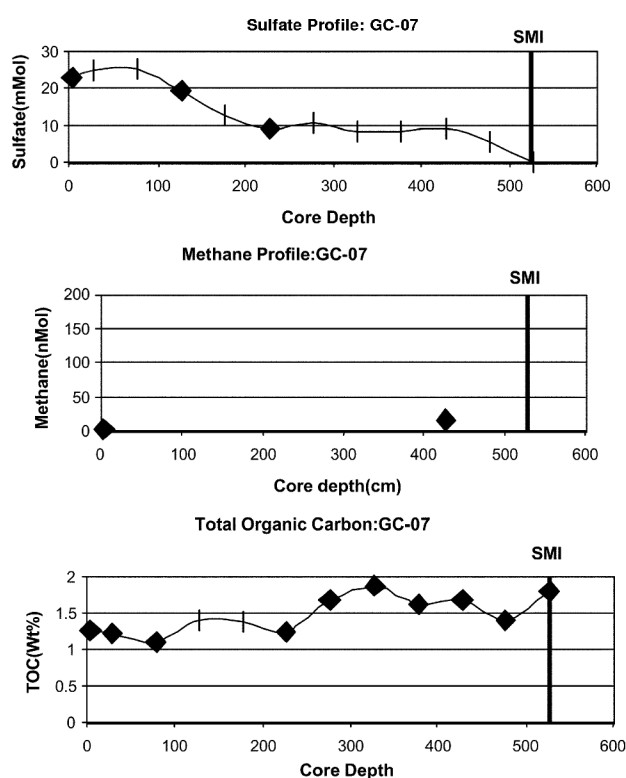


**Figure 4.** Down core variations of sulphate in pore water, and methane and TOC in sediments (Location GC-07).

**Table 1.** Carbonate mineralogy, carbon and oxygen isotope compositions (isotopic compositions are in permil relative to PDB). Sulphate, methane TOC and concentrations through core GC-7

Sample no.	Carbonate sampling depth (cm)	Carbonate mineral	$\delta^{13}\text{C}$ (‰)	$\delta^{18}\text{O}$ (‰)
GC-07	227.5	High-Mg calcite	-51.6	3.6
GC-10	132.5	High-Mg calcite	-48.8	4.2
GC-13	247.5	Aragonite	-50.0	4.5

suggest supply of methane to the shallow sediments, and subsequent bacterially mediated methane oxidation, sulphate reduction and carbonate precipitation. Presence of BSR-like structures at 200–300 m depth, gas up-thrust and pock-mark structures around the surveyed locations (Figure 1) suggest the possibility of deeper source of methane gas, presumably from the hydrate zone. However, the role of early diagenetic methane cannot be underestimated in the present scenario. Observed depletion in sulphate concentration with depth with an appreciable methane enrichment can best be explained by the coupled sulphate reduction-anaerobic methane oxidation mechanism<sup>12,25–29</sup>. Presence of pyrite framboids along with the carbonate precipitates corroborates a sulphate reducing pore water<sup>30</sup>. The zone of overlap of these two components is also known as sulphate methane interface<sup>25,31</sup>. This rapid sulphate depletion, together with the appreciable concentrations of interstitial methane, and relatively high levels of total organic carbon (TOC) suggest anaerobic oxidation condition. Methane oxidation in this zone generally results in very high bicarbonate enrichment (10–100 times the sea water alkalinity<sup>2</sup>), which causes precipitation of different carbonate minerals depending on saturation state and presence/absence of interfering anions<sup>32</sup>. We have recorded high magnesian calcite from cores GC-07 and GC-10 whereas aragonite has been recorded from GC-13, which suggest contrasting pore fluid chemistry. High magnesian calcite precipitation is thought to be favoured by low sulphate and high phosphate concentrations, whereas high sulphate and low phosphate concentrations favour aragonite dominance<sup>6,33</sup>. Carbon and oxygen isotopic compositions of the authigenic carbonate phases reported here falls well within the composition range ( $\delta^{13}\text{C} = -51.6$  to  $-48.8$ ‰ and  $\delta^{18}\text{O} = 3.6$  to  $4.5$ ‰) of methane-derived carbonate<sup>8,9,34</sup>. Both biogenic ( $-50$  to  $-110$ ‰) and thermogenic methane ( $-50$  to  $-20$ ‰) are characterized by highly depleted carbon isotopic compositions. The dissimilarity in isotopic compositions of bacterial and thermogenic  $\text{CH}_4$  accumulations is related to several factors including precursor organic compounds, the difference in type and magnitude of kinetic isotope effects involved, and to the generally higher temperatures for the thermogenic generation of hydrocarbons<sup>35</sup>. In the present study, presence of pyrite, organic-rich sediment and definite evidence of sulphate reduction suggest anaerobic oxidation of methane. Bacterial anaerobic oxidation of methane results in  $^{12}\text{C}$  enriched  $\text{HCO}_3^-$  pool. Authigenic carbonate precipitates preserve this bicarbonate carbon isotope signature. In contrast to the methane production zone,  $\delta^{13}\text{C}$  of residual methane in the AOM-sulphate reduction zone shows relative enrichment in  $^{13}\text{C}$  and narrowing of  $\Delta\delta_{\text{CO}_2-\text{CH}_4}$ . Figure 5 shows the probable range of the carbon isotopic composition of precursor methane as  $-55$  to  $-78$ ‰ ( $\epsilon_c = \sim 5$  to  $30$ ‰) for carbonates. The inferred  $\delta^{13}\text{C}_{\text{CH}_4}$  might lower owing to incorporation of seawater bicarbonate ( $\delta^{13}\text{C} \sim 0$ – $2$ ‰) in the dispersed carbonate phases. The carbon isotopic range

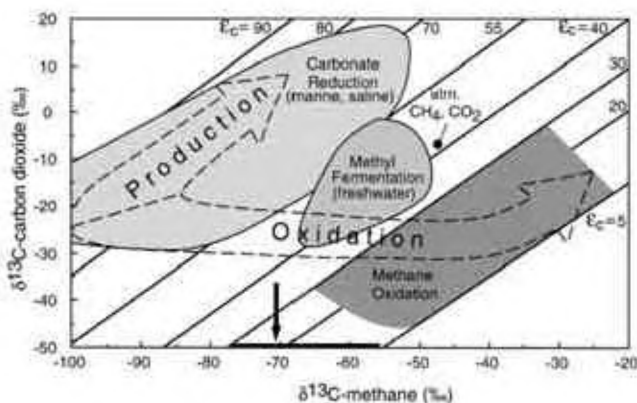


**Figure 5.** Combination plot of  $\delta^{13}\text{C}_{\text{CH}_4}$  and  $\delta^{13}\text{C}_{\text{CO}_2}$  with isotope fractionation line (after ref. 35). Possible range of  $\delta^{13}\text{C}_{\text{CH}_4}$  for the residual methane based on the carbon isotopic composition of carbonates from KG basin cores is indicated by arrow.

for the precursor methane typically suggests a biogenic origin<sup>35</sup>. The oxygen isotope composition of authigenic carbonates is a function of seawater/pore water temperature and mineralogy, which affect oxygen isotope fractionation. Assuming the pore water temperature at 1–2 m sediment depth, same as that of the sea water (4.5°C at 1400–1500 m), the calculated  $\delta^{18}\text{O}$  of aragonite<sup>36</sup> shows 0.8‰ depletion relative to the measured value (at seawater  $\delta^{18}\text{O} = 0\text{‰}$  SMOW). Similarly, for calcite<sup>37</sup> the calculated  $\delta^{18}\text{O}$  is 0.6 to 1.2‰ depleted relative to the measured value. Variable  $^{18}\text{O}$  enrichment in methane-derived carbonates has been reported by several workers<sup>6,33</sup> and can be attributed to  $^{18}\text{O}$  enrichment in the formational water itself, assuming carbonate crystallization in equilibrium with the formational water. Decomposition of gas hydrate and advection of  $^{18}\text{O}$  enriched pore water<sup>33</sup> is one of the other possibilities, although direct evidence for such a process is wanting. Further work is in progress to achieve a comprehensive understanding of the process.

## Conclusions

Presence of dispersed authigenic carbonate precipitates has been reported from three sediment cores from the K–G basin. The cores are located at water depth of 1400 to 1500 m. Studies on the fluid chemistry show down-core depletion in sulphate and enrichment in methane concentrations. This variation can be attributed to bacterially-mediated sulphate reduction and methane oxidation. Presence of pyrite framboids conforms to the anaerobic pore fluid condition. Enrichment of pore water alkalinity brought about by anaerobic oxidation of methane (AOM) resulted in the precipitation of carbonate mineral phases, which is characteristic of the anaerobic methane oxidation zone. Aragonite and high magnesian calcite crystals isolated from these cores supports this contention. The carbonate minerals show a range of morphological characters, viz.

ehedral, acicular and botryoidal crystals, and calcified biofilms, etc. Variation in pore water fluid chemistry, like sulphate and phosphate concentrations and saturation states may be primary controlling factors for aragonite and high magnesian calcite precipitation. Highly depleted carbonate carbon isotopic composition supports methane-derived carbonates. Biogenic origin for the precursor methane in the sediment has been tentatively suggested. Although geophysical investigations in this region point towards the presence of methane gas hydrates at depth, it remains inconclusive if this is the source of methane at shallow depths which is responsible for the observed geochemical processes. Early diagenetic methane production/consumption cannot be ruled out.

1. Botz, R., Faber, E., Whiticar, M. and Brooks, J. M., Authigenic carbonates in sediments from the Gulf of Mexico. *Earth Planet. Sci. Lett.*, 1988, **88**, 263–272.
2. Rodriguez, N. M., Paull, C. K. and Borowski, W. S., Zonation of authigenic carbonates within gas hydrate-bearing sedimentary sections on the Blake Ridge: Offshore Southeastern North America. In *Proc. Ocean Drilling Program, Sci. Results*, 2000, **164**, 301–312.
3. Kulm, L. D. *et al.*, Error in X-ray diffraction estimates of dolomite in carbonate rocks: causes and cures. *Bull. Am. Assoc. Petrol. Geol.*, 1979, **63**, 488.
4. Bohrmann, G., Greinert, J., Suess, E. and Torres, M., Authigenic carbonates from Cascadia Subduction Zone and their relation to gas hydrate stability. *Geology*, 1998, **26/7**, 647–650.
5. Stakes, D. S., Orange, D., Paduan, J. B., Salamy, K. A. and Maher, N., Cold-seeps and authigenic carbonate formation in the Monterey Bay, California. *Mar. Geol.*, 1999, **159**, 93–109.
6. Greinert, J., Bohrmann, G. and Suess, E., Gas hydrate-associated carbonates and methane-venting at Hydrate Ridge: Classification and distribution and origin of authigenic lithologies. *Natural gas hydrates: occurrence, distribution, and dynamics* (eds Paull, C. K. and Dillon, P. W.), *Geophys. Monogr.*, 2001, **124**, 99–113.
7. Han, M. W. and Suess, E., Subduction-induced pore fluid venting and the formation of authigenic carbonates along the Cascadia continental margin: Implications for the global Ca-cycle. *Palaeogeogr. Palaeoclimatol. Palaeoecol.*, 1989, **71**, 97–118.
8. Whiticar, M. J. and Faber, E., Methane oxidation in sediment and water column environments – Isotopic evidence. In *Advances in Organic Geochemistry* (eds Leythaeuser, D. and Rullkötter, J.), 1986, vol. 10, pp. 759–768.
9. Suess, E. and Whiticar, M. J., Methane-derived  $\text{CO}_2$  in pore fluids expelled from the Oregon Subduction Zone. *Palaeogeogr. Palaeoclimatol. Palaeoecol.*, 1989, **71**, 119–136.
10. Hovland, M., Talbot, M. R., Qvale, H., Olaussen, S. and Aasberg, L., Methane-related carbonate cements in pockmarks of the North Sea. *J. Sediment. Petrol.*, 1987, **57**, 881–892.
11. Roberts, H. H., Aharon, P. and Walsh, M. M., Cold-seep carbonates of the Louisiana continental slope-to-basin floor. In *Carbonate Microfabrics* (eds Rezel, R. and Lavoie, D. L.), Springer-Verlag, Berlin, 1993, pp. 95–104.
12. Ritger, S., Carson, B. and Suess, E., Methane-derived authigenic carbonates formed by subduction-induced pore-water expulsion along the Oregon/Washington margin. *Geol. Soc. Am. Bull.*, 1987, **98**, 147–156.
13. Raiswell, R., Chemical model for the origin of minor limestone-shale cycles by anaerobic methane oxidation. *Geology*, 1988, **16**, 641–644.

14. Blair, N. E. and Aller, R. C., Anaerobic methane oxidation on the Amazon shelf. *Geochim. Cosmochim. Acta*, 1995, **59**, 3707–3715.
15. Paull, C. K., Chanton, J. P., Neumann, A. C., Coston, J. A. and Martens, C. S., Indicators of methane-derived carbonates and chemosynthetic organic carbon deposits: Examples from the Florida Escarpment. *Palaios*, 1992, **7**, 361–375.
16. Von Rad, U., Roesch, H., Berner, U., Geyh, M., Marchig, V. and Schulz, H., Authigenic carbonates derived from oxidized methane vented from the Makran accretionary prism off Pakistan. *Mar. Geol.*, 1996, **136**, 55–77.
17. Thiel, V., Peckmann, J., Seifert, R., Wehrung, P., Reitner, J. and Michaelis, W., Highly isotopically depleted isoprenoids: molecular markers for ancient methane venting. *Geochim. Cosmochim. Acta*, 1999, **63**, 3959–3966.
18. Orphan, V. J., House, C. H., Hinrichs, K.-U., McKeegan, K. D. and DeLong, E. F., Methane-derived carbonates and authigenic pyrite from the northwestern Black Sea. *Mar. Geol.*, 2001, **177**, 484–487.
19. Hovland, M. and Judd, A. G., *Seabed Pockmarks and Seepages. Impact on Geology, Biology and Marine Environment* (eds Hovland, M. and Judd, A. G.), Graham and Trotman, London, 1988.
20. Hovland, M., Talbot, M., Qvale, H., Olausson, S. and Aasbø, L., Methane-related carbonate cements in pockmarks of the North Sea. *J. Sediment. Petrol.*, 1987, **57**, 881–892.
21. Rao, C. N., Sedimentation, stratigraphy, and petroleum potential of Krishna–Godavari Basin, East Coast of India. *Bull. Am. Assoc. Petrol. Geol.*, 2001, **85**, 623–643.
22. Ramana, M. V., Ramprasad, T., Desa, M., Sathe, A. V. and Sethi, A. K., Gas hydrate related proxies inferred from multidisciplinary investigations in the India off-shore areas. *Curr. Sci.*, 2006, **91**, 183–189.
23. Fabre, E. and Stahl, W., Analytical procedure and results of an isotope geochemical surface survey in an area of the British North Sea–Petroleum Geochemical and Exploration of Europe. *Spec. Publ. Geol. Soc. London*, 1983, pp. 51–63.
24. Wakeel, E. L. and Riley, J. P., The determination of organic carbon in marine muds. *J. Con. Int. Explor. Mer.*, 1957, **22**, 180–183.
25. Reeburgh, W. S., Anaerobic methane oxidation: rate depth distribution in Skan Bay sediments. *Earth Planet. Sci. Lett.*, 1980, **47**, 345–352.
26. Iversen, N. and Jørgensen, B. B., Anaerobic methane oxidation rates at the sulphate-methane transition in marine sediments from Kattegat and Skagerrak (Denmark). *Limnol. Oceanogr.*, 1985, **30**, 944–955.
27. Borowski, W. S., Paull, C. K. and Ussler, W. III., Marine pore-water sulphate profiles indicate *in situ* methane flux from underlying gas hydrate. *Geology*, 1996, **24**, 655–658.
28. Wallmann, K. *et al.*, Quantifying fluid flow, solute mixing, and biogeochemical turnover at cold vents of the eastern Aleutian subduction zone. *Geochim. Cosmochim. Acta*, 1997, **61/24**, 5209–5219.
29. Aharon, P., Graber, E. R. and Roberts, H. H., Dissolved carbon and  $\delta^{13}\text{C}$  anomalies in the water column caused by hydrocarbon seeps on the northwestern Gulf of Mexico slope. *Geo-Mar. Lett.*, 1992, **12**, 33–40.
30. Berner, R. A., Sedimentary pyrite formation. *Am. J. Sci.*, 1970, **268**, 1–23.
31. Borowski, W. S., Paull, C. K. and Ussler, W. III., Global and local variations of interstitial sulphate gradients in deep water, continental margin sediments: Sensitivity to the underlying methane and gas hydrates. *Mar. Geol.*, 1999, **159**, 131–154.
32. Morse, J. W. and Mackenzie, F. T., Geochemistry of sedimentary carbonates. *Dev. Sedimentol.*, 1990, **48**, 707.
33. Aloisi, G., Pierre, C., Rouchy, J.-M., Foucher, J.-P., Woodside, J. and the MEDINAUT Scientific Party, Methane-related authigenic carbonates of eastern Mediterranean Sea mud volcanoes and their possible relation to gas hydrate destabilization. *Earth Planet. Sci. Lett.*, 2000, **184**, 321–338.
34. Jørgensen, N. O., Methane-derived carbonate cementation of marine sediments from the Kattegat, Denmark: geochemical and geological evidence. *Mar. Geol.*, 1992, **103**, 1–13.
35. Whiticar, M. J., Carbon and hydrogen isotope systematics of bacterial formation and oxidation of methane. *Chem. Geol.*, 1999, **161**, 291–314.
36. Grossman, E. L. and Ku, T.-L., Carbon and oxygen carbon isotope fractionation in biogenic aragonite: temperature effects. *Chem. Geol.*, 1986, **59**, 59–74.
37. Anderson, T. F. and Arthur, M. A., Stable isotopes of oxygen and carbon and their application to sedimentologic and paleo-environmental problems. In *Stable Isotopes in Sedimentary Geology* (eds Arthur, M. A. *et al.*), 1983 I-1-I-1-151, SEPM short course no. 10.

**ACKNOWLEDGEMENTS.** We thank Dr Satish Shetye, Director for providing facilities to publish this work. We acknowledge the help from Dr P. Sanyal of Physical Research Laboratory, Ahmedabad for stable isotope measurements. This research was funded by National Gas Hydrate Programme (NGHP). K.M. thanks Dr V. P. C. Rao and Dr M. V. Ramana for valuable inputs. We also thank the anonymous referees for their meticulous corrections to improve the manuscript. This is NIO contribution No. 4109.

Received 28 November 2005; revised accepted 7 June 2006